

Comparison of Cluster, Slab, and Analytic Potential Models for the Dimethyl Methylphosphonate (DMMP)/TiO₂(110) Intermolecular Interaction

Li Yang,[†] Daniel Tunega,[‡] Lai Xu,[§] Niranjana Govind,^{||} Rui Sun,[§] Ramona Taylor,[⊥] Hans Lischka,[§] Wibe A. DeJong,^{||} and William L. Hase^{*,§}

[†]Technical Institute of Physics and Chemistry, Chinese Academy of Sciences, Beijing 100190, China

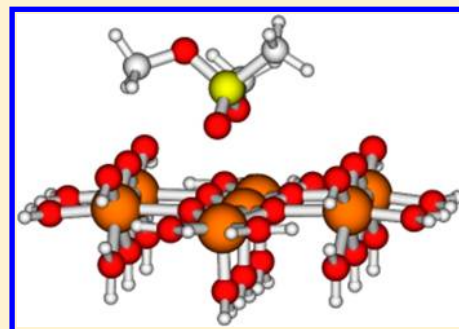
[‡]Institute of Soil Research, University of Natural Resources and Life Sciences, Peter-Jordan-Straße 82b, 1190 Vienna, Austria

[§]Department of Chemistry and Biochemistry, Texas Tech University, Lubbock, Texas 79409-1061, United States

^{||}Environmental Molecular Science Laboratory, Pacific Northwest National Laboratory, Richland, Washington 99352, United States

[⊥]Spectral Sciences, Inc., 4 Fourth Avenue, Burlington, Massachusetts 01803-3304, United States

ABSTRACT: In a previous study (*J. Phys. Chem. C* **2011**, *115*, 12403), cluster models for the TiO₂ rutile(110) surface and MP2 calculations were used to develop an analytic potential energy function for dimethyl methylphosphonate (DMMP) interacting with this surface. In the work presented here, this analytic potential and MP2 cluster models are compared to DFT “slab” calculations for DMMP interacting with the TiO₂(110) surface and with DFT cluster models for the TiO₂(110) surface. The DFT slab calculations were performed with the PW91 and PBE functionals. The analytic potential gives DMMP/TiO₂(110) potential energy curves in excellent agreement with those obtained from the slab calculations. The cluster models for the TiO₂(110) surface, used for the MP2 calculations, were extended to DFT calculations with the B3LYP, PW91, and PBE functionals. These DFT calculations do not give DMMP/TiO₂(110) interaction energies that agree with those from the DFT slab calculations. Analyses of the wave functions for these cluster models show that they do not accurately represent the HOMO and LUMO for the surface, which should be 2p and 3d orbitals, respectively, and the models also do not give an accurate band gap. The MP2 cluster models do not accurately represent the LUMO, and that they give accurate DMMP/TiO₂(110) interaction energies is apparently fortuitous, arising from their highly inaccurate band gaps. To address this issue, accurate cluster models, consisting of 7, 10, and 15 Ti-atoms and that have the correct HOMO and LUMO properties, are proposed. The Ti₇-cluster model gives a DMMP + TiO₂ rutile(110) potential energy curve, determined with DFT, which is consistent with those for the MP2 cluster and DFT slab calculations and with the analytic potential energy function. DFT-D calculations, with a dispersion correction, give DMMP + TiO₂ rutile(110) binding energies ~10–15 kcal/mol stronger than those obtained from pure DFT. The DMMP + TiO₂ rutile(110) binding energy is found to depend on the size of the model used to represent the TiO₂(110) surface. The work presented here illustrates that care must be taken in “constructing” cluster models that accurately model surfaces.



I. INTRODUCTION

Cluster models are widely used in quantum chemistry studies to represent surfaces and their interactions with molecules. Stoichiometric cluster models have been used to represent alumina surfaces and their interactions with alkane^{1,2} and water³ molecules, and with the chemical warfare agents (CWAs) Sarin and VX^{4,5} and the CWA surrogate dimethyl methylphosphonate (DMMP). Interactions of trichlorophosphate (TCP), DMMP, and Sarin with the amorphous SiO₂ surface have been investigated with cluster models.⁶ A number of studies have been performed in which TiO₂ cluster models have been used to represent the TiO₂ rutile(110) surface and its interactions with molecules. These studies include Ti₇O₁₄ with H₂O;^{7,8} Ti₇O₉, Ti₇O₁₈, and Ti₇O₃₀ with organic molecules;⁹ and TiO₅H₆ with small molecules representing functional groups in peptides.¹⁰ Different cluster sizes

containing 1, 2, 4, 6, and 17 Ti-atoms were used to study the interactions of catechol and water with the TiO₂ anatase(101) surface.¹¹ In the above studies, it was important to choose a cluster that has the proper interfacial structure and atomic charges. Carefully constructed TiO₂ cluster models have also been used to study the effects of dopants on the UV/vis properties.¹² The embedded cluster approach^{3,8,9,12,13} has also been used.

In recent work, we used cluster models to study the intermolecular interaction of DMMP with the TiO₂ rutile(110) surface.¹⁴ The calculations were performed at the MP2 level of theory with two basis sets, 6-31++G** (6-31G** for Ti) and

Received: May 18, 2013

Revised: July 20, 2013

Published: August 5, 2013

aug-cc-pVDZ (6-311+G** for Ti). The three clusters TiO_5H_6 , $\text{Ti}_3\text{O}_{13}\text{H}_{14}$, and $\text{Ti}_{11}\text{O}_{40}\text{H}_{36}$ were used for the calculations. From the results of these calculations, an analytic intermolecular potential between DMMP and the $\text{TiO}_2(110)$ surface was developed, written as a sum of two-body interactions between the atoms of DMMP and those of the TiO_2 surface.

For the work presented here, two additional calculations were performed to compare with the above MP2 cluster calculations for the DMMP/rutile(110) surface.¹⁴ For one, DFT “slab” calculations were performed to determine DMMP/rutile(110) potential energy curves to compare with those reported for the MP2 cluster calculations. For the second, elements of the MP2 cluster calculations were repeated but using the DFT/B3LYP model theory instead of MP2. Of interest are the similarities and differences in the MP2 cluster, DFT “slab”, and DFT/B3LYP cluster models of the DMMP/rutile(110) intermolecular interaction. In addition, more accurate cluster models^{9,12,13} that take into account the local bonding environment are discussed and presented. These models are based on a covalent embedding procedure for which Ti_xO_y clusters are terminated with suitably chosen pseudohydrogen saturators identified as Z-atoms.

II. COMPUTATIONAL METHODS AND RESULTS

II.A. Slab Calculations for DMMP/ $\text{TiO}_2(110)$. *II.A.1. Procedure.* Two different DFT periodic slab calculations were performed for the potential energy of the DMMP/rutile(110) system. For one DMMP, $\text{O}=\text{P}(\text{CH}_3)(\text{OCH}_3)_2$ was held fixed in its optimized structure, and potential energy curves for DMMP interacting with the surface were calculated for specific DMMP orientations and interaction sites on the surface. There was no geometry optimization for either DMMP or the surface. These calculations follow those reported for the two orientations in Figures 7–9 of ref 14, with one additional orientation. Depictions of these three orientations are given in Figure 1. The part of the rutile(110) surface included was chosen to illustrate the interaction site on the surface. For the second calculation, the potential energy release for DMMP association with the $\text{TiO}_2(110)$ surface was determined. This

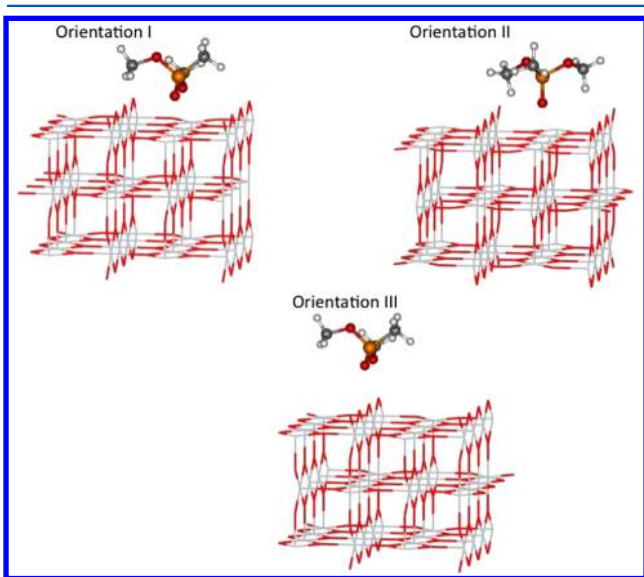


Figure 1. Three orientations considered for DMMP interacting with the $\text{TiO}_2(110)$ surface. Details of the orientations are given in the text.

energy is the difference in the energy of the optimized DMMP–rutile(110) system, with DMMP and rutile(110) held rigid, and the total energy of individually optimized DMMP and rutile(110). This is the same approach as was used in our previous study employing the Ti -, Ti_3 -, and Ti_{11} -cluster models for rutile(110).¹⁴ If the geometry of the DMMP–cluster system was optimized with DMMP attached, the resulting relaxation/deformation of the cluster would depend on the cluster size. To ensure that this did not artificially affect the DMMP interaction energy, rigid models were employed as described above. The same approach was used for the slab calculations so that they could be compared to the cluster calculations.

The periodic DFT calculations were performed with the Vienna ab initio simulation package (VASP),^{15–19} using the periodic supercell model for the TiO_2 slab. The slab has a thickness of ~ 9 Å, contains 3 Ti planes, and consists of 48 $[\text{TiO}_2]$ units. Its construction was based on the known bulk structure of TiO_2 .²⁰ The parameters of the computational cell are $a = 50$, $b = 11.836$, $c = 12.994$ Å, and $\alpha = \beta = \gamma = 90^\circ$. The calculations were performed with two DFT functionals, PW91²¹ and PBE.²² The plane wave cutoff was set to 400 eV, and SCF convergence was set to 0.0001 eV. All calculations were performed using the projected augmented wave (PAW)²³ approach at the Γ point. PAW atomic pseudopotentials¹⁹ were used for both the PW91 and the PBE functionals.

II.A.2. Results and Comparison with Energies Given by the Analytic Potential Energy Function. Potential energy curves are given in Figure 2 for DMMP interacting with a DFT “slab” model of the TiO_2 rutile(110) surface for the three orientations in Figure 1. The curves were calculated using the PW91 and PBE functionals as described above. For orientation I, the double bond O atom of DMMP approaches a 5-coordinated Ti atom along the Ti–O axis, and, at the same time, one of the methoxy O atoms of DMMP approaches another 5-coordinated Ti atom. Thus, both the Ti–O(P) and the Ti–O(C) interactions are emphasized. For orientation II, the double bond O atom of DMMP approaches a 5-coordinated Ti atom with collinear P–O and Ti–O axes, and only the Ti–O(P) interaction is emphasized. For orientation III, the P atom approaches above one of the 6-coordinated Ti atoms, with O(P) approaching above the middle bridging O atom and a methoxy O atom approaching above a side bridging O atom.

As shown in Figure 2, the PW91 and PBE functionals give nearly identical potential energy curves, with orientation I giving a deeper potential energy curve than orientation II and a repulsive potential energy curve for orientation III. Fitting the potential energy curves with cubic spline functions gives PW91 and PBE potential energy minimum parameters V_o , R_o of -44.0 kcal/mol, 2.20 Å and -42.1 kcal/mol, 2.22 Å, respectively, for orientation I and V_o , R_o of -33.4 kcal/mol, 2.24 Å and -31.8 kcal/mol, 2.25 Å, respectively, for orientation II. If the minimum energy structures for orientations I and II are optimized, with both DMMP and the TiO_2 slab held rigid, the resulting respective PW91 and PBE V_o , R_o parameters are of -45.9 kcal/mol, 2.20 Å and -44.1 kcal/mol, 2.20 Å for orientation I and -34.2 kcal/mol, 2.25 Å and -33.3 kcal/mol, 2.24 Å for orientation II.

DFT slab calculations have been performed of the structure and dynamics of liquid water on TiO_2 rutile(110).²⁴ The binding and dissociation energies of water are found to depend on the number of layers in the slab. DFT calculations have also shown that the surface properties of thin TiO_2 rutile(110) films depend on the number of layers in two-dimensional slab

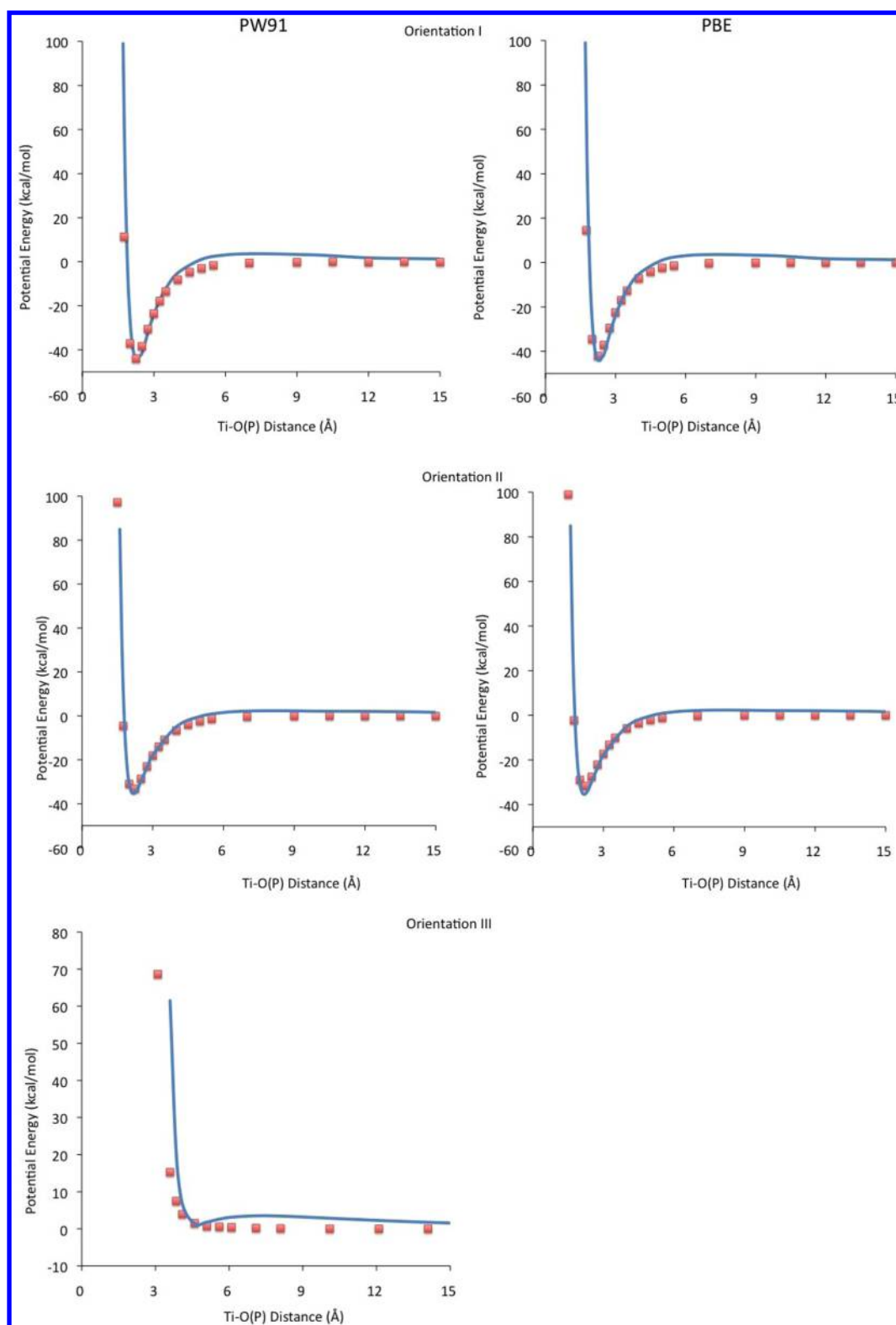


Figure 2. DFT “slab” calculations of potential energy curves for DMMP interacting with the $\text{TiO}_2(110)$ surface for the three orientations in Figure 1. The structures of DMMP and $\text{TiO}_2(110)$ are held rigid and are not optimized. The results of the DFT slab calculations, PW91 (left column) and PBE (right column), are given by the points. The potential energy curves from the analytic function are given by the solid curves. The Ti–O(P) distance is the distance of the O-atom of $\text{O}=\text{P}$ from the top layer of Ti-atoms.

models of the surface.²⁵ Thus, it is important to determine if the above DMMP/rutile(110) interaction energies, obtained with the 3-layer model, change if a model with more layers is used. A test was made for orientation II in Figure 1, using a 4-

layer model and the PW91 functional. Figure 3 shows that the interaction potential energy curves for the 3- and 4-layer models are nearly identical. A cubic spline fit to the 4-layer curve gives potential energy minimum parameters $V_0 = -33.6$

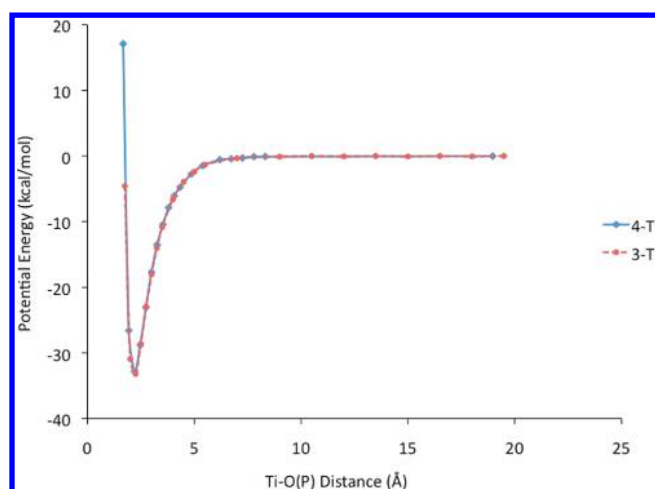


Figure 3. Comparison of DMMP/TiO₂ rutile(110) potential energy curves for orientation II in Figure 1, using the DFT/PW91 “slab” model with 3-layers (red curve) and 4-layers (blue curve). The Ti–O(P) distance is defined in the caption to Figure 2.

kcal/mol and $R_0 = 2.11$ Å. These parameters are nearly the same as those above for the 3-layer model. The 3-layer model is apparently sufficient for calculating accurate DMMP/rutile(110) interaction energies.

As discussed above, the slab model for rutile(110) was held rigid for the calculations. For the DFT calculations of water interacting with slab models of the rutile(110) surface,²⁵ properties of the interaction of water with the surface were found to depend on the relaxation of the surface and whether an “even” or “odd” number of surface layers were included in the calculation. For the current study, with a rigid surface, such an “even” or “odd” effect was not observed. In future work, it would be of interest to consider additional rutile(110) slab models and determine if such an effect is observed for the DMMP interaction if relaxation of the slab model is allowed.

In previous work, utilizing MP2 calculations and cluster models,¹⁴ an analytic intermolecular potential energy function written as a sum of two-body terms was developed for DMMP interacting with the TiO₂ rutile(110) surface. The potential energy curves given by this potential for orientations I–III are plotted in Figure 2, where they are compared to those for the PW91 and PBE 3-layer “slab” calculations. The analytic potential energy function curves were calculated in the same manner as those for the slab calculations; that is, DMMP and the TiO₂ rutile(110) surface were kept rigid and brought together as defined for orientations I, II, and III. The overall agreement between the DFT and analytic function potential energy curves is quite good. For orientation III, the analytic function has a shallow minimum of 1.4 kcal/mol, with a barrier of 3.5 kcal/mol to access this minimum. In comparison, the DFT curves are purely repulsive for this orientation. The analytic potential gives V_0 , R_0 values of -44.2 kcal/mol, 2.30 Å and -35.3 kcal/mol, 2.17 Å for orientations I and II, respectively, which are in quite good reasonable agreement with the above DFT values. The conclusion from the comparisons in Figure 2 is that the MP2 cluster models give a DMMP/rutile(110) interaction potential similar to that given by the DFT “slab” calculations.

For comparison with the cluster calculations, discussed in the next section, it is of interest to have the HOMO, LUMO, and Fermi-level energies for the DFT slab calculations. The PW91

values for these energies are given in Table 1 for the potential energy minima of the DMMP/rutile(110) orientations I and II

Table 1. HOMO, LUMO, and Fermi-Level Energies for the PW91 Slab Calculations^a

system	HOMO	LUMO	Fermi-level	HOMO–LUMO gap
DMMP/TiO ₂ –I	–4.71	–3.79	–4.527	0.92
DMMP/TiO ₂ –II	–4.87	–3.95	–4.605	0.92
isolated TiO ₂	–5.26	–4.39	–5.075	0.87

^aThe energies are in eV. Orientations I and II are defined in Figure 1, and the energies are for the optimized structures of these orientations.

and for isolated rutile(110). As discussed below, the MP2 cluster models correctly describe the HOMO, but not the LUMO. The agreement between the DMMP/rutile(110) interaction energies of the MP2 cluster and DFT slab models arises from a fortuitous large separation between the HOMO and LUMO orbitals.

II.B. Comparison of DFT and MP2 Model Cluster Calculations for the DMMP/TiO₂ Rutile(110) Intermolecular Interaction Potential. In previous work,¹⁴ MP2 theory was used to calculate interaction energies between DMMP and the TiO₅H₆, Ti₃O₁₃H₁₄, and Ti₁₁O₄₀H₃₆ clusters as successively more accurate models of the DMMP/TiO₂ rutile(110) interaction. As discussed above, the analytic intermolecular potential energy function derived from these calculations gives DMMP/rutile(110) potential energy curves in good agreement with those determined from DFT “slab” calculations. Here, we compare B3LYP, PBE, and PW91 DFT calculations with these previous MP2 calculations of DMMP interacting with Ti-clusters. The DFT calculations were performed with the Gaussian03 software package.²⁶ The same basis set, 6-31++G** (6-31 G* for Ti), was used for all of the calculations.

DFT and MP2 energies for DMMP binding to the Ti-clusters are compared in Table 2. The calculations are for the specific DMMP/Ti-cluster potential energy curves described in

Table 2. Comparison of MP2 and DFT Energies for DMMP Binding with Ti-Clusters^a

Ti-cluster	$R_{\text{Ti–O(P)}}^c$	binding energy ^b			
		MP2	B3LYP	PW91	PBE
TiO ₅ H ₆	2.20	–19.9	–19.2		
Ti ₃ O ₁₃ H ₁₄	2.10	–34.2	–30.7	–39.6	–36.0
Ti ₁₁ O ₄₀ H ₃₆ –I	2.50	–28.6	–19.5	–20.1	–19.0
Ti ₁₁ O ₄₀ H ₃₆ –II	2.50	–19.4	–12.8	–13.9	–13.0

^aThe structures of the Ti-clusters and the orientations of DMMP for binding to the clusters are given in ref 14. For the Ti₁₁-cluster, there are two orientations, I and II. The basis set used for the calculations is 6-31++G**, with 6-31G** for Ti. ^bThe binding energies are given in kcal/mol. A BSSE correction was included in the binding energies as discussed previously¹³ for the MP2 calculations. ^c $R_{\text{Ti–O(P)}}$ is the distance in angstroms of the O-atom of O=P from the top layer of Ti-atoms of the clusters. The same $R_{\text{Ti–O(P)}}$ distance is used for each of the theories to compare the calculated binding energies. These distances are close to the distances for the minima in the potential energy curves; see ref 14. At the MP2 potential minima for the Ti₃ and Ti₁₁ clusters, the V_0 and $R_{\text{Ti–O(P)}}$ are: Ti₃, -34.3 kcal/mol, 2.07 Å; Ti₁₁ (orientation I), -28.9 kcal/mol, 2.41 Å; Ti₁₁ (orientation II), -19.6 kcal/mol, 2.44 Å.

ref 14. To compare the binding energies for the different theories, the same Ti–O(P) distance was used for each theory. These distances are close to those for the potential energy minima of the curves. For the Ti_3 -cluster, the different DFT functionals give different values for the binding energy. The PBE functional gives a binding energy close to the MP2 value, while B3LYP and PW91 give energies that are lower and higher, respectively. Important results in Table 2 are the similar DFT binding energies for the Ti_{11} -cluster, which are 30–35% smaller than the MP2 binding energy. As discussed above, the MP2 binding energies are very similar to those found with the DFT slab models for the TiO_2 rutile(110) surface. In the following, the origin of the different DMMP/rutile(110) binding energies, as given by the DFT cluster and slab models, is considered.

To explain the inconsistency between the minima of the MP2 and DFT potential energy curves for the DMMP/Ti-cluster models, an investigation was made to explore the orbital character of the TiO_5H_6 , $\text{Ti}_3\text{O}_{13}\text{H}_{14}$, and $\text{Ti}_{11}\text{O}_{40}\text{H}_{36}$ clusters. These calculations were performed with the NWChem software package.²⁷ The HOMO–LUMO character of pure TiO_2 is O-2p (HOMO) and Ti-3d (LUMO). The calculated band gap of TiO_2 (rutile) is about 3.2 eV for the bulk and about 2.5–3.0 eV for the surface.^{28,29} The experimental band gaps for the bulk and surface are ~ 3.0 eV.^{28,29} Periodic DFT calculations with the B3LYP and PBE functionals predict about 3.2 and 2.0 eV, respectively, for the band gap.^{28,29}

Table 3 shows the HOMO–LUMO character and band gap for the three clusters used to model the interaction of DMMP

Table 3. HOMO–LUMO Character and Gaps for the Three Clusters TiO_5H_6 , $\text{Ti}_3\text{O}_{13}\text{H}_{14}$, and $\text{Ti}_{11}\text{O}_{40}\text{H}_{36}$

	cluster		
	TiO_5H_6	$\text{Ti}_3\text{O}_{13}\text{H}_{14}$	$\text{Ti}_{11}\text{O}_{40}\text{H}_{36}$
		B3LYP	
HOMO	O-2p	O-2p	O-2p, Ti-4s hybrid
LUMO	O-2p, Ti-3d, H-s	O-2p, Ti-3d, Ti-3p, H-s	Ti-3d, Ti-4s
gap (eV)	~ 5.0	~ 2.1	~ 2.1
		HF	
HOMO	O-2p	O-2p	O-2p(major), Ti-4s
LUMO	Ti-4s, O-2s, H-s	Ti-4s, Ti-3d, H-s, O-2s, Ti-3p	Ti-4s, Ti-3p
gap (eV)	~ 12.2	~ 9.0	~ 9.1

interacting with the TiO_2 surface. The HF HOMO orbitals for the cluster show the proper O-2p character, but the LUMO does not have the correct character. The reason the HF-MP2 results are consistent with the DFT slab calculations is because the band gaps are very large, which keeps the unoccupied states sufficiently far away. The agreement with periodic DFT slab calculations is apparently completely fortuitous.

The B3LYP, PW91, and PBE DFT calculations for the Ti clusters are expected to yield the same orbital character for the HOMO and LUMO as found for the DFT slab calculations. To investigate this, the HOMO and LUMO orbitals of the clusters were characterized for the B3LYP calculations as shown in Table 3. We find the proper O-2p HOMO character for the TiO_5H_6 and $\text{Ti}_3\text{O}_{13}\text{H}_{14}$ clusters, but the HOMO character is completely different and incorrect for the $\text{Ti}_{11}\text{O}_{40}\text{H}_{36}$ cluster. For each of the three clusters, the LUMO is incorrect. The

mixed nature of the HOMO in the Ti_{11} -cluster is the most likely reason the DFT energies for DMMP binding with this cluster are inconsistent. A plausible reason for the wrong HOMO–LUMO character is the complete H passivation, which does not take the local bonding environment and the proper valencies of the Ti and O atoms into consideration.¹² We discuss a procedure to account for this in the next section. Proper termination of the surface, with pseudohydrogens, has been discussed in previous work by Casarin and co-workers and others.^{9,12,13,30–32}

II.C. Proposed More Accurate Cluster Models. To improve the structure of the cluster models, new cluster models were developed as shown in Figure 4. They are $\text{Ti}_7\text{O}_{27}\text{Z}_{36}$, $\text{Ti}_{10}\text{O}_{36}\text{Z}_{36}\text{H}_8$, and $\text{Ti}_{15}\text{O}_{54}\text{Z}_{51}\text{H}_{14}$, and their properties were characterized with the NWChem software package.²⁷ Their design is based on a covalent embedding procedure where

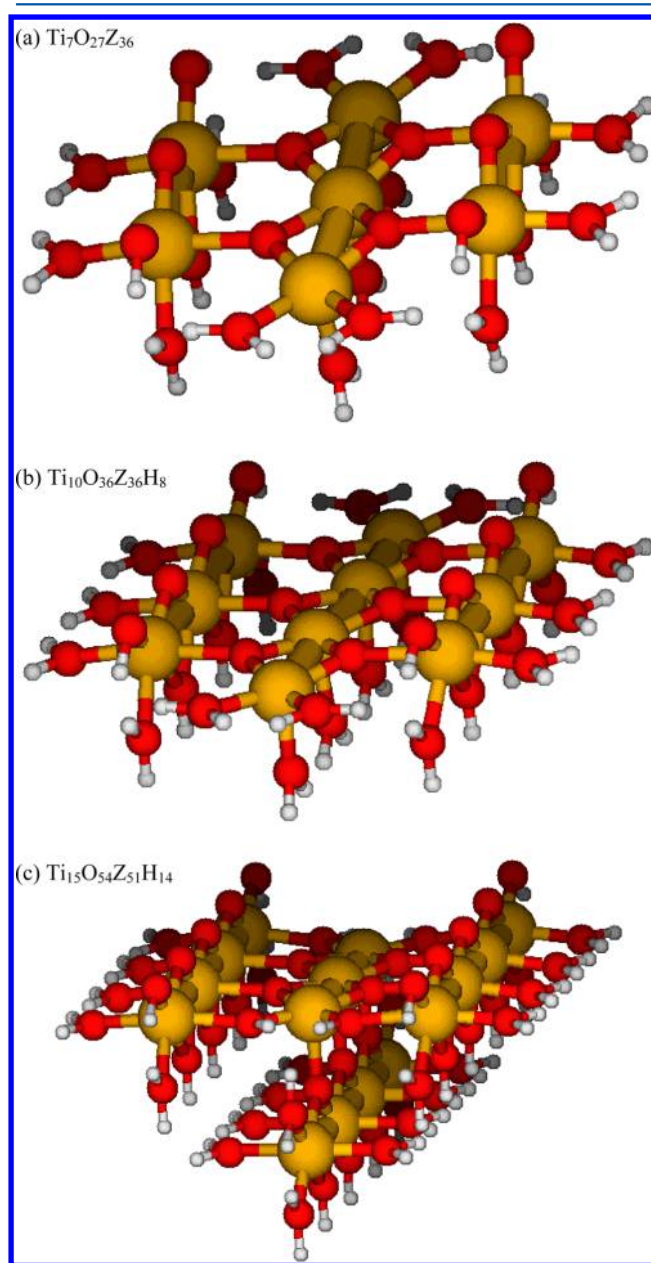


Figure 4. Structures of the three new Ti-clusters to model DMMP interacting with the TiO_2 (110) surface.

Ti_xO_y clusters are terminated using a set of suitably chosen pseudohydrogen saturators Z whose charges are calculated using the formal charges of the Ti (+4) and O (−2) atoms as well as their coordination in bulk TiO₂ rutile.^{9,12,13} The Ti atoms in the bulk rutile structure are coordinated by six O atoms, while the O atoms are coordinated by three Ti atoms. Within the formal charge picture, each Ti atom contributes 2/3 of an electron to each O atom that coordinates it. This determines the charges for passivating the Ti and O dangling bonds. The pseudohydrogens passivating the O dangling bond have a charge of $Z = 2/3$ |e|, while the pseudohydrogens passivating the Ti dangling bonds have a charge of $Z = -2/3$ |e|. This embedding procedure maintains the charge neutrality of the system as well as satisfying the valencies of Ti and O. The structures for the three clusters we considered were completely optimized. All of the interior atoms were allowed to move freely, whereas the pseudohydrogens as well as the atoms directly connected to them were kept fixed. Clusters constructed using this approach have been successfully used to study the adsorption of small molecules^{9,13} as well as the excited-state properties of pure and N-doped TiO₂.¹² The basis sets used for these clusters consist of LANL2DZ³³ for the Ti-atoms, Stuttgart RCL-ECP³⁴ for the O-atoms, and 3-21G for the pseudohydrogens, whose charge is $-1/3$. The hybrid DFT functional B3LYP was used for these calculations. Previous work has shown³⁵ that it gives much better band gaps than do pure-GGA functionals such as PW91 and PBE.

As shown in Table 4, each of the clusters has a dominant O-2p in the HOMO and a dominant Ti-3d in the LUMO. This is

Table 4. Character and Band Gaps for the Three New Clusters Ti₇O₂₇Z₃₆, Ti₁₀O₃₆Z₃₆H₈, and Ti₁₅O₅₄Z₅₁H₁₄^a

	cluster		
	Ti ₇ O ₂₇ Z ₃₆	Ti ₁₀ O ₃₆ Z ₃₆ H ₈	Ti ₁₅ O ₅₄ Z ₅₁ H ₁₄
HOMO	O-2p	O-2p	O-2p
LUMO	Ti-3d	Ti-3d	Ti-3d
gap (eV)	~3.2 eV	~4.0 eV	~2.1 eV

^aThe results were obtained from B3LYP calculations.

consistent with the periodic slab DFT calculations. The band gaps for the surface cluster models can vary from 2 to 4 eV because of the nonuniqueness of the model. The gap may even oscillate as the number of layers is increased for the cluster. This pattern is also observed with slab calculations.²⁵ For bulk cluster models, with the passivation approach used here, the gaps do not vary much because the models are fully coordinated.¹² For cluster models of the surface, the size of the gap is affected by the number of under-coordinated atoms. However, the character of the gap should always be HOMO-O 2p and LUMO-Ti 3d.

Rittner et al.^{36,37} have suggested that a cluster at least the size of Ti₉O₁₈ is required to accurately represent the electronic structure of the Ti adsorption site as well as that of the five adjacent oxygen atoms. As shown in Table 4, for the detailed Ti₇O₂₇Z₃₆, Ti₁₀O₃₆Z₃₆H₈, and Ti₁₅O₅₄Z₅₁H₁₄ cluster models proposed here, Ti₇O₂₇Z₃₆ with seven Ti-atoms gives electronic properties similar to those for the larger clusters. However, as discussed in section III, a larger cluster model is needed to accommodate all of the interactions and calculate an accurate energy for DMMP interacting with the rutile(110) surface.

To investigate the nature of the potential energy for DMMP interacting with these clusters, the minimum potential energy

was calculated for DMMP interacting with the Ti₇O₂₇Z₃₆ cluster in orientation I. DFT/PW91 was used for the calculation, with the same basis set for DMMP as described in Table 2, 6-311++G**. The basis set for the cluster is described above. The complete potential energy curve was not calculated, and only the potential energy V_0 and distance R_0 for the potential minimum were determined (R is the distance of the O-atom of O=P from the top Ti-layer of the cluster). The calculations were performed as for those in Figure 2, with DMMP and the Ti₇O₂₇Z₃₆ cluster held rigid and fixed in orientation I as shown in Figure 5. The values for V_0 and R_0 are

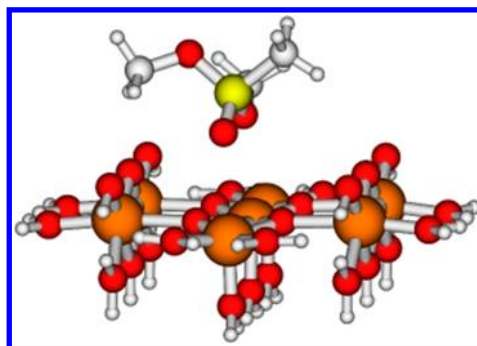


Figure 5. Depiction of DMMP interacting with the Ti₇O₂₇Z₃₆ cluster in orientation I.

−24.6 kcal/mol and 2.51 Å. This binding energy is similar to, but somewhat smaller than, the MP2 value of −28.9 kcal/mol in footnote c of Table 2 for the Ti₁₁-cluster in orientation I. BSSE corrections^{38,39} were not included in the cluster calculations with pseudohydrogens.

The analytic potential energy function developed for DMMP interacting with the TiO₂ rutile(110) surface¹⁴ was used to determine the potential energy minimum for DMMP interacting with the Ti₇O₂₇Z₃₆ cluster in orientation I and to compare to the above DFT/PW91 calculation. The potential energy function's values for V_0 and R_0 are −26.8 kcal/mol and 2.69 Å, in good agreement with the above DFT/PW91 results. This comparison indicates the DMMP + TiO₂ rutile(110) surface analytic potential energy function, developed from MP2 calculations and the previous Ti-cluster models,¹⁴ provides a good representation of the interaction between DMMP and these new Ti-cluster models, as well as for DMMP interacting with slab models of the TiO₂ rutile(110) surface as shown above.

II.D. DFT-D Calculations. In recent research,⁴⁰ DFT has been modified by including a dispersion contribution in the electron density. It is of interest to determine if these DFT-D methods significantly alter the above DFT energies for DMMP interacting with the models for the TiO₂ rutile(110) surface. This analysis was made for the periodic slab and Ti₇O₂₇Z₃₆ models of the rutile surface. The DFT-D calculations were performed with DFT/PW91-D2.⁴¹ Orientation II (Figure 1) and the 3-layer model were used for the slab calculation, and the PW91 and PW91-D2 potential energy curves are compared in Figure 6, where it is seen that the PW91-D2 calculation gives a substantially deeper potential energy curve. As given above, V_0 and R_0 for the PW91 calculation are −33.4 kcal/mol and 2.24 Å. In contrast, PW91-D2 gives −46.4 kcal/mol and 2.12 Å for these values. These calculations were also performed with the PBE functional (not shown), and the resulting V_0 , R_0 values are −31.8 kcal/mol, 2.25 Å and −44.9 kcal/mol, 2.14 Å for PBE

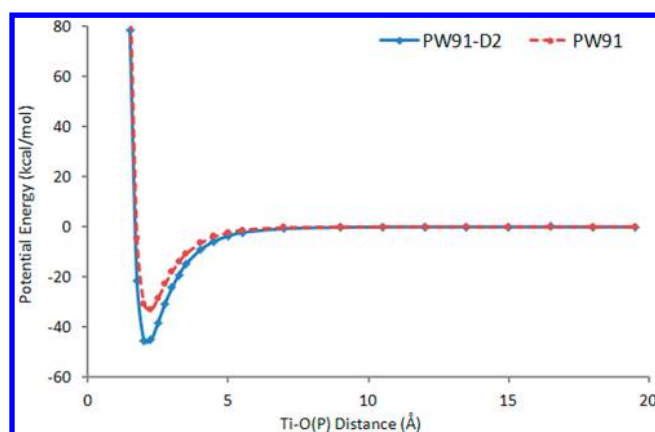


Figure 6. Comparison of DMMP/TiO₂ rutile(110) potential energy curves for orientation II in Figure 1, using the 3-layer periodic slab model with DFT/PW91 (red curve) and DFT/PW91-D2 (blue curve). The Ti–O(P) distance is defined in the caption to Figure 2.

and PBE-D2, respectively. The dispersion correction increases the binding energy by ~ 13 kcal/mol.

In a similar manner, the PW91-D2 potential energy minimum was determined for DMMP interacting with the new Ti₇O₂₇Z₃₆ cluster to compare with the PW91 minimum. For the PW91-D2 calculation, V_o , R_o are -39.0 kcal/mol, 2.44 Å, as compared to the PW91 values of -24.6 kcal/mol, 2.51 Å given above. The dispersion correction increases the binding energy by ~ 14 kcal/mol, similar to the above result for the slab calculation.

III. COMPARISON WITH PREVIOUS CALCULATIONS OF DMMP AND SARIN BINDING ENERGIES ON METAL OXIDES

In previous work,^{5,6,42–45} energies have been calculated for DMMP, O=P(CH₃)(OCH₃)₂, the similar molecule Sarin, O=P(F)(CH₃)[(CH₃)₂CHO], and small molecules binding to metal oxide surfaces. The electronic structure method used for these calculations is DFT, without the “-D” modification of the DFT functional, and both cluster and periodic slab models were employed to represent the metal oxide surfaces. The results of these calculations are summarized in Table 5. Of the surfaces Al₂O₃, TiO₂, and *a*SiO₂, the calculations indicate that DMMP and Sarin bind strongest with Al₂O₃ and the weakest with *a*SiO₂. The presence of H₂O on the oxide surface significantly decreases the DMMP and Sarin binding energies.

As shown in Table 5, the previous DFT/B3LYP/cc-pVDZ calculations⁴⁴ for DMMP/TiO₂ rutile(110) used a Ti₁₁O₄₀H₃₂ cluster model, which is similar to the Ti₁₁O₄₀H₃₆ model considered in Table 2 and for which MP2 gives accurate results as described above. The binding energy of -31.2 kcal/mol for the Ti₁₁O₄₀H₃₂ cluster is similar to the MP2 value of -28.9 for orientation I of our Ti₁₁O₄₀H₃₆ cluster. For our Ti₇O₂₇Z₃₆ cluster discussed in section II.C, the DFT/PW91 binding energy for orientation I is -24.6 kcal/mol and somewhat lower than the above values. The analytic potential energy function gives -26.8 kcal for the DMMP-Ti₇O₂₇Z₃₆ binding energy. The DFT/PW91 periodic slab calculations discussed in section II.A give binding energies of -44.0 and -33.4 kcal/mol for orientations I and II, respectively, values larger than those obtained with the Ti₁₁-cluster models. Our analytic potential energy function gives similar binding energies of -44.2 and -35.3 kcal/mol for DMMP adsorption on the TiO₂ rutile slab.

Table 5. Previous Calculations of Absorption Energies for Metal Oxide Surfaces

system	ΔE_{ad}^a	method	ref
TiO ₂ –H ₂ O	-21.7^b	DFT/GGA/PW91 ^e	42
TiO ₂ –H ₃ PO ₃	-29.1	periodic DFT ^e	43
TiO ₂ –DMMP	-31.2	DFT/B3LYP/cc-pVDZ ^f	44
<i>a</i> SiO ₂ –DMMP	-20.0	DFT ONIOM ^g	6
Al ₂ O ₃ –DMMP	-41.4	periodic DFT ^f	5
TiO ₂ –DMMP(H ₂ O)	-6.9^c	DFT/B3LYP/cc-pVDZ ^f	44
TiO ₂ –DMMP(H ₂ O)	$-10.0^{d,d}$	DFT/B3LYP/6-31G* ^{h,f}	44
Al ₂ O ₃ –DMMP(H ₂ O)	$-23.2^{d,d}$	periodic DFT ^f	5
<i>a</i> SiO ₂ –DMMP(H ₂ O)	$-4.7^{d,d}$	ReaxFF MD ^e	45
TiO ₂ –Sarin	-30.6	DFT/B3LYP/cc-pVDZ ^f	44
<i>a</i> SiO ₂ –Sarin	-21.4	DFT ONIOM ^e	6
Al ₂ O ₃ –Sarin	-39.8	periodic DFT ^f	5
TiO ₂ –Sarin(H ₂ O)	-7.2^c	DFT/B3LYP/cc-pVDZ ^f	44
TiO ₂ –Sarin(H ₂ O)	$-13.4^{d,d}$	DFT/B3LYP/cc-pVDZ ^f	44
Al ₂ O ₃ –Sarin(H ₂ O)	$-21.9^{d,d}$	periodic DFT ^f	5

^aThe classical absorption energy in kcal/mol, without zero-point energy corrections. ^bMolecular water at the full monolayer coverage. ^cMolecular water. ^dDissociated water. ^eNo BSSE and zero-point energy (ZPE) corrections. ^fBSSE correction, but no ZPE correction.

These results show that the DMMP binding energy increases as -25 , ~ -30 , and -44 kcal/mol for the Ti₇ cluster, Ti₁₁ cluster, and TiO₂(110) slab models, respectively. Apparently, the DMMP binding energy becomes stronger as the size of the model used to represent the TiO₂ rutile(110) surface increases. This is supported by the calculations with the analytic potential energy function.

IV. SUMMARY

In previous work,¹⁴ the TiO₅H₆, Ti₃O₁₃H₁₄, and Ti₁₁O₄₀H₃₆ clusters were used as models for the TiO₂ rutile(110) surface. MP2 calculations, utilizing these cluster models, were then performed to develop an analytic potential energy function for dimethyl methylphosphonate (DMMP) interacting with this surface.¹⁴ In the work presented here, it is found that this MP2-based analytic potential gives DMMP/rutile(110) potential energy curves in excellent agreement with those obtained from DFT “slab” calculations performed with the PW91 and PBE functionals. To compare with these DFT slab calculations, DFT calculations were also performed for DMMP interacting with the TiO₅H₆, Ti₃O₁₃H₁₄, and Ti₁₁O₄₀H₃₆ clusters. The B3LYP, PW91, and PBE functionals were used for these calculations. These DFT calculations do not give DMMP/Ti-cluster interaction energies that agree with those for the previous MP2 calculations and, as a result, do not give DMMP/rutile(110) potential energy curves that agree with those from the DFT slab calculations. Analyses of the DFT wave functions for the TiO₅H₆, Ti₃O₁₃H₁₄, and Ti₁₁O₄₀H₃₆ clusters show that they do not accurately represent the HOMO and LUMO for the surface, which should be O-2p and Ti-3d orbitals, respectively. They also do not give an accurate band gap as compared to that for the surface. The MP2 cluster models do not accurately represent the LUMO, and that they give accurate DMMP/TiO₂ rutile(110) interaction energies is apparently fortuitous, arising from their highly inaccurate band gaps. This work illustrates that much care must be taken in “constructing” cluster models that accurately model surfaces, a point that has also been emphasized in previous work.^{13,30–32}

Accurate cluster models consisting of 7, 10, and 15 Ti-atoms, and that have the correct HOMO and LUMO properties, are proposed. The potential energy curve was calculated for DMMP interacting with this Ti_7 -cluster, and the binding energy is similar to, but somewhat smaller than, the MP2 value for the Ti_{11} -cluster studied previously.¹⁴ The analytic potential energy function for DMMP interacting with the TiO_2 rutile(110) surface, developed from the MP2 calculations,¹⁴ gives a good representation of the DFT potential energy for DMMP interacting with the new Ti_7 -cluster.

DFT-D calculations, with a dispersion correction,⁴⁰ were performed to compare to the MP2 and DFT calculations. The DFT-D2 model theory⁴¹ gives a DMMP + TiO_2 rutile(110) binding energy ~ 10 – 15 kcal/mol stronger than the DFT value for both the slab and the new Ti_7 -cluster models for the surface.

There are inconsistencies in the relationships between the MP2 and DFT calculations for DMMP interacting with models of TiO_2 rutile(110) surfaces. In comparing the MP2 and DFT calculations, it is important to recognize that both are model representations of the exact electronic structure theory. As pointed out above, the analytic potential energy function developed from the MP2 calculations, for DMMP interacting with Ti -cluster models of the surface, fits the DFT calculations for DMMP interacting with both the slab model and the new Ti_7 -cluster model for the surface. Given the differences between the cluster models for the MP2 calculations and the slab and cluster models for the DFT calculations, this agreement does not appear to be fortuitous. It is consistent with the suggestion⁴⁶ that the adsorption interaction between DMMP and oxide surfaces is predominantly the formation of a dative bond between a lone-pair of atoms on the O-atom of the $\text{P}=\text{O}$ group and an unoccupied orbital of a Ti-atom of the surface. Such an interaction is described by both MP2 and DFT, as well as additional electrostatic interactions between DMMP and the surface. The inconsistency arises with the DFT-D calculations. DFT does not include dispersion, and “-D” is an empirical correction to account for this interaction.⁴⁰ The inclusion of “-D” in the DFT calculations increases the DMMP adsorption energy by 40% and 60%, respectively, for the slab and Ti_7 -cluster models for the TiO_2 rutile(110) surface. Because MP2 includes dispersion, this result brings into question the meaning of the above agreement between the MP2 and DFT calculations. It also questions the suggestion⁴⁶ that the DMMP/ TiO_2 interaction is dominated by a dative bond between DMMP and the surface. However, there are uncertainties concerning the accuracy of the empirical “-D” correction⁴¹ used here for the DMMP TiO_2 oxide surface interaction. Recent work⁴⁷ shows that often there are strong renormalization (screening) effects in solids due to electrodynamic response. For organic/inorganic interfaces, this screening can substantially reduce the “-D” C_6 coefficient as compared to gas-phase molecules. The conclusion that may be drawn from the current study is that the MP2, DFT, and DFT-D calculations are in qualitative agreement.

The accurate cluster models developed here, consisting of 7, 10, and 15 Ti-atoms, as well as the slab model could be used to calculate potential energy curves for CWAs such as Sarin and VX interacting with the TiO_2 rutile(110) surface. It would be of interest to compare their interaction energies with those for DMMP. The rutile(110) surface and face contains four types of atoms, that is, 5- and 6-fold coordinated Ti atoms, 3-fold coordinated bulk O-atoms, and 2-fold coordinated bridging O-atoms. The DMMP/rutile(110) analytic potential was

developed by fitting two-body potentials between these four atom types for rutile and the different atoms of DMMP. An interesting question is whether these two-body potentials and their parameters may be used to describe the interaction of DMMP with other TiO_2 surfaces. This may be investigated by calculating potential energy curves for DMMP interacting with slab models of different TiO_2 surfaces. The rutile(100) and anatase(101) surfaces^{43,48,49} have the same four types of atoms as does rutile(110), and the DMMP/rutile(110) analytic potential may be applicable to these two surfaces. Because the TiO_2 anatase and brookite surfaces have different surface features as compared to rutile, it is doubtful that the DMMP/rutile(110) analytic potential will be transferable to the(110) counterparts of these polymorphs. Nevertheless, it would still be of interest to test this possibility with slab DFT calculations for the different surfaces.

The adsorption interaction between a molecule as DMMP, containing a $\text{P}=\text{O}$ group, and the $\gamma\text{-Al}_2\text{O}_3$ surface has been described as the formation of a donor bond between the O-atom of $\text{P}=\text{O}$ and a surface Al-atom.⁴⁶ For different surface cluster models, a linear relationship is found between the adsorption energy and the difference in the energy of the HOMO of the molecule and LUMO of the surface. For the work presented here, the interaction between DMMP and TiO_2 rutile(110) surface is accurately represented by a sum of two-body interactions between the DMMP atoms and those of the surface, for which the O-atoms of the $\text{P}=\text{O}$ and $\text{P}-\text{O}$ groups all have attractive interactions with the surface Ti-atoms. This analytic potential accurately represents the interaction between DMMP and the TiO_2 slab model as well as Ti -cluster models of different sizes. In future work, it would certainly be of interest to consider a potential energy function for DMMP interacting with slab and cluster models of TiO_2 surfaces in which there is a donor bond between the O-atom of $\text{P}=\text{O}$ and a surface Ti-atom, as well as two-body interactions between the remaining DMMP atoms and surface atoms.

AUTHOR INFORMATION

Corresponding Author

*Phone: 806-742-3152. E-mail: bill.hase@ttu.edu.

Notes

The authors declare no competing financial interest.

ACKNOWLEDGMENTS

This material is based upon work supported by the Army Research Office under Contract HDTRA1-07-C-0098 and the Robert A. Welch Foundation under Grant D-0005. Support was also provided by the High-Performance Computing Center (HPCC) at Texas Tech University, under the direction of Dr. Philip W. Smith. The research was also performed using EMSL, a national scientific user facility sponsored by the Department of Energy's Office of Biological and Environmental Research and located at Pacific Northwest National Laboratory. This work was also supported by a grant from the German Research Foundation, priority program SPP 1315, Project GE1676/1-1. We acknowledge the Texas Advanced Computing Center (TACC) at The University of Texas at Austin for providing HPC resources that have contributed to the research results reported within this Article.

REFERENCES

- (1) Bolton, K.; Bosio, S. B. M.; Hase, W. L.; Schneider, W. F.; Hass, K. C. Comparison Between United and Explicit Atom Models for Simulating Alkane Chains Physisorbed on an Aluminum Terminated (0001) α -Aluminum Oxide Surface. *J. Phys. Chem. B* **1999**, *103*, 3885–3895.
- (2) Sawilowsky, E. F.; Schlegel, H. B.; Hase, W. L. Structures and Energies for Methane Complexed with Alumina Clusters. *J. Phys. Chem. A* **2000**, *104*, 4920–4927.
- (3) Wittbrodt, J. M.; Hase, W. L.; Schlegel, H. B. An ab Initio Study of the Interaction of Water with Cluster Models of the Aluminum Terminated (0001) α -Aluminum Oxide Surface. *J. Phys. Chem. B* **1998**, *102*, 6539–6548.
- (4) Bermudez, V. M. Quantum-Chemical Study of the Adsorption of DMMP and Sarin on γ -Al₂O₃. *J. Phys. Chem. C* **2007**, *111*, 3719–3728.
- (5) Bermudez, V. M. Computational Study of Environmental Effects in the Adsorption of DMMP, Sarin, and VX on γ -Al₂O₃: Photolysis and Surface Hydration. *J. Phys. Chem. C* **2009**, *113*, 1917–1930.
- (6) Bermudez, V. M. Computational Study of the Adsorption of Trichlorophosphate, Dimethyl Methylphosphonate, and Sarin on Amorphous SiO₂. *J. Phys. Chem. C* **2007**, *111*, 9314–9323.
- (7) Stefanovich, E. V.; Truong, T. N. Ab Initio Study of Water Adsorption on TiO₂(110): Molecular Adsorption versus Dissociative Chemisorption. *Chem. Phys. Lett.* **1999**, *299*, 623–629.
- (8) Bandura, A. V.; Sykes, D. G.; Shapovalov, V.; Truong, T. N.; Kubicki, J. D.; Evarestov, R. A. Adsorption of Water on the TiO₂ (Rutile) (110) Surface: A Comparison of Periodic and Embedded Cluster Calculations. *J. Phys. Chem. B* **2004**, *108*, 7844–7853.
- (9) Sushko, M. L.; Gal, A. Yu.; Shluger, A. L. Interaction of Organic Molecules with the TiO₂ (110) Surface: Ab Initio Calculations and Classical Force Fields. *J. Phys. Chem. B* **2006**, *110*, 4853–4862.
- (10) Carravetta, V.; Monti, S. Peptide-TiO₂ Surface Interaction in Solution by Ab Initio and Molecular Dynamics Simulations. *J. Phys. Chem. B* **2006**, *110*, 6160–6169.
- (11) Redfern, P. C.; Zapol, P.; Curtiss, L. A.; Rajh, T.; Thurnauer, M. C. Computational Studies of Catechol and Water Interactions with Titanium Oxide. *J. Phys. Chem. B* **2003**, *107*, 11419–11427.
- (12) Govind, N.; Lopata, K. A.; Rousseau, R. J.; Andersen, A.; Kowalski, K. Visible Light Absorption of N-Doped TiO₂ Rutile Using (LR/RT)-TDDFT and Active Space EOMCCSD Calculations. *J. Phys. Chem. Lett.* **2011**, *2*, 2696–2701.
- (13) Casarin, M.; Maccato, C.; Vittadini, A. Molecular Chemisorption on TiO₂(110): A Local Point of View. *J. Phys. Chem. B* **1998**, *102*, 10745–10752.
- (14) Yang, L.; Taylor, R.; de Jong, W. A.; Hase, W. L. A Model DMMP/TiO₂(s) Intermolecular Potential Energy Function Developed from Ab Initio Calculations. *J. Phys. Chem. C* **2011**, *115*, 12403–12413.
- (15) Kresse, G.; Hafner, J. Ab Initio Molecular Dynamics for Liquid Metals. *J. Phys. Rev. B* **1993**, *47*, 558–561.
- (16) Kresse, G.; Hafner, J. Ab Initio Molecular-Dynamics Simulation of the Liquid-Metal–Amorphous-Semiconductor Transition in Germanium. *Phys. Rev. B* **1994**, *49*, 14251–14269.
- (17) Kresse, G.; Fürthmüller, J. Efficiency of Ab-initio Total Energy Calculations for Metals and Semiconductors Using a Plane-wave Basis Set. *J. Comput. Mater. Sci.* **1996**, *6*, 15–50.
- (18) Kresse, G.; Fürthmüller, J. Efficient Iterative Schemes for Ab Initio Total-energy Calculations Using a Plane-wave Basis Set. *Phys. Rev. B* **1996**, *54*, 11169–11186.
- (19) Kresse, G.; Joubert, D. From Ultrasoft Pseudopotentials to the Projector Augmented-Wave Method. *Phys. Rev. B* **1999**, *59*, 1758–1775.
- (20) Zhang, Z.; Fenter, P.; Cheng, L.; Sturchio, N.; Bedzyk, M. J.; Predota, M.; Bandura, A.; Kubicki, J. D.; Lvov, S. N.; Cummings, P. T.; et al. Ion Adsorption at the Rutile–Water Interface: Linking Molecular and Macroscopic Properties. *Langmuir* **2004**, *20*, 4954–4969.
- (21) Perdew, J. P.; Wang, Y. Accurate and Simple Analytic Representation of the Electron-gas Correlation Energy. *Phys. Rev. B* **1992**, *45*, 13244–13249.
- (22) Perdew, J. P.; Burke, K.; Ernzerhof, M. Generalized Gradient Approximation Made Simple. *Phys. Rev. Lett.* **1996**, *77*, 3865–3868.
- (23) Blöchl, P. E. Projector Augmented-wave Method. *Phys. Rev. B* **1994**, *50*, 17953–17979.
- (24) Liu, L.-M.; Zhang, C.; Thornton, G.; Michaelides, A. Structure and Dynamics of Liquid Water on Rutile TiO₂(110). *Phys. Rev. B* **2010**, *82*, 161415–(1)–161415–(4).
- (25) Bredow, H.; Giordano, L.; Cinquini, F.; Pacchioni, G. Electronic Properties of Rutile TiO₂ Ultrathin Films: Odd-even Oscillations with the Number of Layers. *Phys. Rev. B* **2004**, *70*, 035419(1)–035419(6).
- (26) Frisch, M. J.; Trucks, G. W.; Schlegel, H. B.; Scuseria, G. E.; Robb, M. A.; Cheeseman, J. R.; Montgomery, J. A., Jr.; Vreven, T.; Kudin, K. N.; Burant, J. C.; et al. *Gaussian 03*, revision B.04; Gaussian, Inc.: Pittsburgh, PA, 2003.
- (27) Valiev, M.; Bylaska, E. J.; Govind, N.; Kowalski, K.; Straatsma, T. P.; van Dam, H. J. J.; Wang, D.; Nieplocha, J.; Apra, E.; Windus, T. L.; de Jong, W. A. NWChem: A Comprehensive and Scalable Open-source Solution for Large Scale Molecular Simulations. *Comput. Phys. Commun.* **2010**, *181*, 1477–1489.
- (28) Labat, F.; Baranek, P.; Domain, C.; Minot, C.; Adamo, C. Density Functional Theory Analysis of the Structural and Electronic Properties of TiO₂ Rutile and Anatase Polytypes: Performances of Different Exchange-Correlation Functionals. *J. Chem. Phys.* **2007**, *126*, 154703–154714.
- (29) Labat, F.; Baranek, P.; Adamo, C. Structural and Electronic Properties of Selected Rutile and Anatase TiO₂ Surfaces: An ab Initio Investigation. *J. Chem. Theory Comput.* **2008**, *4*, 341–352.
- (30) Casarin, M.; Maccato, C.; Vittadini, A. Theoretical Study of the Chemisorption of CO on Al₂O₃(0001). *Inorg. Chem.* **2000**, *39*, 5232–5237.
- (31) Casarin, M.; Maccato, C.; Vittadini, A. A Comparative Study of CO Chemisorption on Al₂O₃ and TiO₂ Nonpolar Surfaces. *J. Phys. Chem. B* **2002**, *106*, 795–802.
- (32) Casarin, M.; Falcomer, D.; Glisenti, A.; Vittadini, A. Experimental and Theoretical Study of the Interaction of CO₂ with α -Al₂O₃. *Inorg. Chem.* **2003**, *42*, 436–445.
- (33) Hay, P. J.; Wadt, W. R. Ab Initio Effective Core Potentials for Molecular Calculations. Potentials for the Transition Metal Atoms Sc to Hg. *J. Chem. Phys.* **1985**, *82*, 270–283.
- (34) Bergner, A.; Dolg, M.; Kuechle, W.; Stoll, H.; Preuss, H. Ab Initio Energy-adjusted Pseudopotentials for Elements of Groups 13–17. *Mol. Phys.* **1993**, *80*, 1431–1441.
- (35) Muscat, J.; Wander, A.; Harrison, N. M. On the Prediction of Band Gaps from Hybrid Functional Theory. *Chem. Phys. Lett.* **2001**, *342*, 397–401.
- (36) Rittner, F.; Fink, R.; Boddenberg, B.; Staemmler, V. Adsorption of Nitrogen on Rutile (110): Ab initio Cluster Calculations. *Phys. Rev. B* **1998**, *57*, 4160–4174.
- (37) Rittner, F.; Boddenberg, B.; Fink, R. F.; Staemmler, V. Adsorption of Nitrogen on Rutile(110). 2. Construction of a Full Five-Dimensional Potential Energy Surface. *Langmuir* **1999**, *15*, 1449–1455.
- (38) Boys, S. F.; Bernardi, F. The Calculation of Small Molecular Interactions by the Differences of Separate Total Energies. Some Procedures with Reduced Errors. *Mol. Phys.* **1970**, *19*, 553–566.
- (39) Newton, M. D.; Kestner, N. R. The Water Dimer: Theory versus Experiment. *Chem. Phys. Lett.* **1983**, *94*, 198–201.
- (40) Wu, Q.; Yang, W. Empirical Correction to Density Functional Theory for van der Waals Interactions. *J. Chem. Phys.* **2002**, *116*, 515–526.
- (41) Grimme, S. Semiempirical GGA-Type Density Functional Constructed with Long-Range Dispersion Correction. *J. Comput. Chem.* **2006**, *27*, 1787–1799.
- (42) Bandura, A. V.; Kubicki, J. D. Derivation of Force Field Parameters for TiO₂-H₂O Systems from ab Initio Calculations. *J. Phys. Chem. B* **2003**, *107*, 11072–11081.
- (43) Raghunath, P.; Lin, M. C. A Computational Study on the Adsorption Configurations and Reactions of Phosphorous acid on

Anatase (101) and Rutile (110) Surfaces. *J. Phys. Chem. C* **2009**, *113*, 8394–8406.

(44) Taylor, R. S.; Cuiang, C.; Shroll, R. M. Determining the Reactivity of Chemical Warfare Agents on Metal Oxide Surfaces via Computational Chemistry. *Proceedings of Chemical and Biological Defense Physical Science and Technology Conference*; New Orleans, LA, Nov. 7–21, 2008.

(45) Quenneville, J.; Taylor, R. S.; van Duin, A. C. T. Reactive Molecular Dynamics Studies of DMMP Adsorption and Reactivity on Amorphous Silica Surfaces. *J. Phys. Chem. C* **2010**, *114*, 18894–18902.

(46) Bermudez, V. M. Energy-level Alignment in the Adsorption of Phosphonyl Reagents on γ -Al₂O₃. *Surf. Sci.* **2008**, *602*, 1938–1947.

(47) (a) Zhang, G.-X.; Tkatchenko, A.; Paier, J.; Appel, H.; Scheffler, M. van der Waals Interactions in Ionic and Semiconductor Solids. *Phys. Rev. Lett.* **2011**, *107*, 245501-(1)–245501-(5). (b) Ruiz, V. G.; Liu, W.; Zojer, E.; Scheffler, M.; Tkatchenko, A. Density-Functional Theory with Screened van der Waals Interactions for the modeling of Hybrid Inorganic–Organic Systems. *Phys. Rev. Lett.* **2012**, *108*, 146103-(1)–146103-(5).

(48) Perron, H.; Domain, C.; Roques, J.; Drot, R.; Simoni, E.; Catalette, H. Optimisation of Accurate Rutile TiO₂ (110), (100), (101) and (001) Surface Models from Periodic DFT Calculations. *Theor. Chem. Acc.* **2007**, *117*, 565–574.

(49) Vittadini, A.; Selloni, A.; Rotzinger, E. P.; Grätzel, M. Structure and Energetics of Water Adsorbed at TiO₂ Anatase (101) and (001) Surfaces. *Phys. Rev. Lett.* **1998**, *81*, 2954–2957.